



Lawrence Berkeley Laboratory

UNIVERSITY OF CALIFORNIA

RECEIVED
LAWRENCE
BERKELEY LABORATORY

MAR 5 1981

LIBRARY AND
DOCUMENTS SECTION

To be submitted to Nuclear Physics A

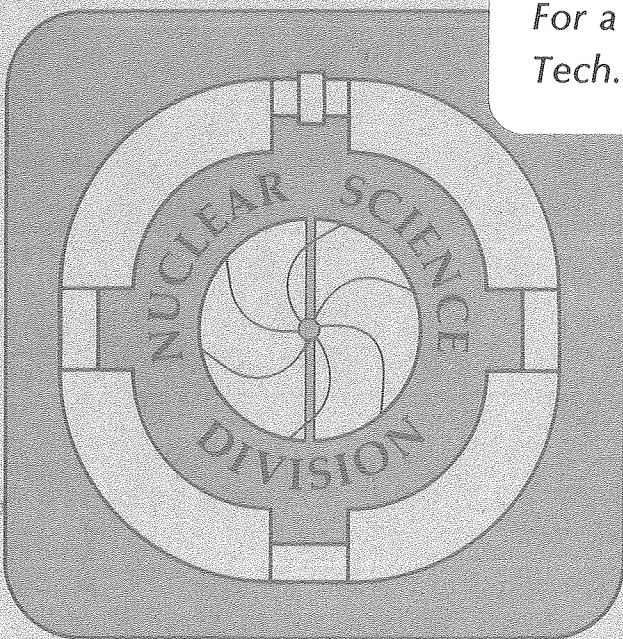
GROUND STATE PROPERTIES OF O^{16} , Ca^{40} AND Ca^{48} IN
A RELATIVISTIC HARTREE THEORY OF NUCLEAR MATTER

J. Boguta

December 1980

TWO-WEEK LOAN COPY

*This is a Library Circulating Copy
which may be borrowed for two weeks.
For a personal retention copy, call
Tech. Info. Division, Ext. 6782.*



LBL-11894
c. 2

DISCLAIMER

This document was prepared as an account of work sponsored by the United States Government. While this document is believed to contain correct information, neither the United States Government nor any agency thereof, nor the Regents of the University of California, nor any of their employees, makes any warranty, express or implied, or assumes any legal responsibility for the accuracy, completeness, or usefulness of any information, apparatus, product, or process disclosed, or represents that its use would not infringe privately owned rights. Reference herein to any specific commercial product, process, or service by its trade name, trademark, manufacturer, or otherwise, does not necessarily constitute or imply its endorsement, recommendation, or favoring by the United States Government or any agency thereof, or the Regents of the University of California. The views and opinions of authors expressed herein do not necessarily state or reflect those of the United States Government or any agency thereof or the Regents of the University of California.

Ground State Properties of O^{16} , Ca^{40} and Ca^{48}
in a Relativistic Hartree Theory of Nuclear Matter*

J. Boguta

Nuclear Science Division
Lawrence Berkeley Laboratory
University of California
Berkeley, CA 94720

Abstract:

A relativistic field theory model of nuclear matter is solved in a Hartree approximation for finite nuclei. We show that the theory predicts small shell effects for the charge density distributions in magic nuclei and is in agreement with recent electron scattering data. The effects of the small component of the relativistic wave function are investigated as well as the role of the isospin dependent force generated by the rho field.

*This work was supported by the Division of Nuclear Physics of the Office of High Energy and Nuclear Physics of the U. S. Department of Energy, under Contract W-7405-ENG-48.

Recently we reported on the ground state and thermally excited states of finite nuclei in a Thomas-Fermi approximation to a relativistic quantum field theory of nuclear matter¹⁾. These calculations were able to reproduce the observed characteristics of finite nuclei such as charge density distributions, level density parameter and rms radii reasonably well in terms of a few, well-understood parameters. The shortcoming of those calculations was the Thomas-Fermi approximation itself, which neglects the shell structure of a nucleus and the effects it has on the ground state properties. One knows that these shell effects are important, though the magnitude of these effects has been the source of considerable uncertainty. Many Hartree-Fock calculations based on two-body nucleon-nucleon interaction have predicted considerable shell influence on the charge density distributions²⁾. Recent experimental data on electron scattering has revealed that these effects are actually not as big as believed³⁾. To account for this fact, one needs quite a sophisticated nuclear model, such as density dependent Hartree-Fock (DDHF)⁴⁾.

The quality of our results in the T-F approximation was sufficiently good that one must ask the question whether shell effects in this model will spoil the T-F picture and eliminate the relativistic quantum field model as a viable phenomenological theory. The purpose of this work is to investigate the ground state properties of O^{16} , Ca^{40} and Ca^{48} nuclei where shell effects would be most important and show that in the Hartree approximation the reported T-F results are improved just where improvement was needed; a shell contribution of correct magnitude to the density distributions together with a correct density falloff at the boundary of the nucleus. We show that the relativistic theory even in its simplest form does not have large shell oscillations for the central nuclear density as predicted by conventional Hartree-Fock calculations.

The relativistic quantum field theory of nuclear matter assumes that nuclear matter saturation is obtained by the interplay of attraction generated by a scalar meson and repulsion generated by a vector meson. The density dependence of these forces is dictated by relativistic covariance. Duerr and Teller exploited these ideas some years ago quite successfully⁵⁾. They were able to predict the energy dependence of the optical potential and the size of spin-orbit splitting in finite nuclei. These ideas were cast in field theory form by Walecka⁶⁾ and extended by Boguta and Bodmer⁷⁾ to include sigma meson self-interactions.

The relativistic quantum field theory of nuclear matter as proposed by Walecka assumes that the nucleon ψ interacts with a scalar meson σ , a vector meson ω_μ , and isovector meson \hat{R}_μ and electromagnetic field A_μ . The Lagrangian for the system is taken to be

$$\begin{aligned} \mathcal{L} = & -\bar{\psi}(\gamma_\mu \partial_\mu + m_n)\psi - \frac{1}{2} ((\partial_\mu \sigma)^2 + m_\sigma^2 \sigma^2) - \frac{1}{4} F_{\mu\nu} F_{\mu\nu} - \frac{1}{4} \vec{G}_{\mu\nu} \cdot \vec{G}_{\mu\nu} \quad (1) \\ & - \frac{1}{4} H_{\mu\nu} H_{\mu\nu} - \frac{1}{2} m_\omega^2 \omega_\lambda \omega_\lambda - \frac{1}{2} m_\rho^2 \hat{R}_\mu \cdot \hat{R}_\mu + ig_\omega \bar{\psi} \gamma_\lambda \psi \omega_\lambda \\ & + ig_\rho \bar{\psi} \gamma_\lambda \hat{\tau} \cdot \hat{R}_\lambda \psi + ie \bar{\psi} \gamma_\mu \frac{(1 + \tau_3)}{2} \psi A_\mu - g_s \bar{\psi} \psi \sigma \end{aligned}$$

where the field tensors $F_{\mu\nu}$, $\vec{G}_{\mu\nu}$, $H_{\mu\nu}$ are given by the usual expression

$$F_{\mu\nu} = \frac{\partial}{\partial X_\mu} \omega_\nu - \frac{\partial}{\partial X_\nu} \omega_\mu \quad (2a)$$

$$\vec{G}_{\mu\nu} = \frac{\partial}{\partial X_\mu} \hat{R}_\nu - \frac{\partial}{\partial X_\nu} \hat{R}_\mu \quad (2b)$$

$$H_{\mu\nu} = \frac{\partial}{\partial X_\mu} A_\nu - \frac{\partial}{\partial X_\nu} A_\mu \quad (2c)$$

and the isotopic spin structure of ψ is

$$\psi = \begin{pmatrix} \psi_p \\ \psi_n \end{pmatrix} \quad (3)$$

In the Lagrangian m_s , m_v and m_n are the masses of the scalar sigma meson, the vector mesons omega and rho, and the nucleon, respectively. The quantum field theory is approximated by the use of the mean field approximation, in which the quantum field operators are replaced by their expectation values $\sigma \rightarrow \langle \sigma \rangle = \sigma_0$, $\omega_\mu \rightarrow \langle \omega_\mu \rangle = \delta_{\mu 0} \omega_0$, $A_\mu \rightarrow \langle A_\mu \rangle = \delta_{\mu 0} A_0$, $R_\mu^{(k)} \rightarrow \langle R_\mu^{(k)} \rangle = \delta_{k0} \delta_{\mu 0} R_0^{(0)}$. The validity of this approximation has not been proven for densities encountered in finite nuclei. Chin has shown that at high densities the mean field approximation becomes accurate⁸⁾. One did not expect the theory to be phenomenologically useful at normal nuclear densities until it was shown by Boguta and Rafelski⁹⁾ that such a theory can indeed approximate the ground state properties of finite nuclei reasonably well. The fact that a relativistic field theory seems to work in describing magic nuclei must be considered as a phenomenological statement. The mean field approximation is, so to speak, a relativistic extension of the shell model and not its justification.

The equations of motion for spherically symmetric nuclei are given by

$$\frac{d^2 \sigma_0}{dr^2} + \frac{2}{r} \frac{d\sigma_0}{dr} = m_s^2 \sigma_0 + g_s (\rho_s^{(n)} + \rho_s^{(p)}) \quad (4a)$$

$$\frac{d^2 \omega_0}{dr^2} + \frac{2}{r} \frac{d\omega_0}{dr} = m_v^2 \omega_0 - g_v (\rho_v^{(n)} + \rho_v^{(p)}) \quad (4b)$$

$$\frac{d^2 R_0^{(0)}}{dr^2} + \frac{2}{r} \frac{dR_0^{(0)}}{dr} = m_v^2 R_0^{(0)} - g_r (\rho_v^{(n)} - \rho_v^{(p)}) \quad (4c)$$

$$\frac{d^2 A_0}{dr^2} + \frac{2}{r} \frac{dA_0}{dr} = e \rho_v^{(p)} \quad (4d)$$

The neutron and proton scalar and vector densities ($\delta_S^{(n)}$, $\delta_S^{(p)}$, $\rho_V^{(n)}$, $\rho_V^{(p)}$) are given by

$$\rho_S = \sum_{\ell} \bar{\psi}_{\ell} \psi_{\ell} \quad (4e)$$

$$\rho_V = \sum_{\ell} \psi_{\ell}^{\dagger} \psi_{\ell} \quad (4f)$$

where $\bar{\psi} = \psi^{\dagger} \gamma_0$ and we sum over all occupied proton and neutron states of the nucleus. The proton and neutron wave functions satisfy the Dirac equation. For spherical geometry they can be written as

$$\psi = \frac{1}{r} \begin{pmatrix} iU(r) \\ V(r) \hat{\sigma} \cdot \hat{n} \end{pmatrix} \Omega_{j\ell m}(\hat{n}) \quad (5)$$

where the functions U and V satisfy the following coupled equations

$$\frac{dU}{dr} = (m_n + E + g_s \sigma - W)V - \frac{K}{r} U \quad (6a)$$

$$\frac{dV}{dr} = (m_n - E + g_s \sigma + W)U + \frac{K}{r} V \quad (6b)$$

with

$$K = \pm(j + \frac{1}{2}) \text{ for } j = \ell \mp \frac{1}{2} \quad (6c)$$

and

$$W = g_V \omega_0 + eA_0 - g_r R_0^{(0)} \quad (7a)$$

$$= g_V \omega_0 + g_r R_0^{(0)} \quad (7b)$$

The solutions of the Dirac equation for small distances ($r \approx 0$) are given by the spherical Bessel functions of the first kind

$$U = Zj_K(Z) \quad K > 0 \quad (8a)$$

$$= Zj_{-1-K}(Z) \quad K < 0 \quad (8b)$$

$$V = \frac{\beta Z}{(E-W)+m^*} j_{K-1}(Z) \quad K > 0 \quad (8c)$$

$$V = \frac{\beta Z}{(E-W)+m^*} j_{-K}(Z) \quad K < 0 \quad (8d)$$

$$\beta = \sqrt{(E - W)^2 + m^{*2}} \quad (8e)$$

$$Z = \beta r \quad (8f)$$

Asymptotically the wave functions are given in terms of modified spherical Bessel functions of the third kind for neutrons and Whittaker functions for the protons, the latter being the solution to the Dirac equation with a static Coulomb potential.

The small distance behavior of the relativistic wave functions is of interest, because it determines the central density distribution in nuclei. For the s-wave states $s_{1/2}$ ($K = -1$) $U \sim j_0(\beta r)$, $V \sim j_1(\beta r)$ while for the p-wave state $p_{1/2}$ ($K = +1$) $U \sim j_1(\beta r)$, $V \sim j_0(\beta r)$. At the origin ($r \approx 0$) the large component of the s-wave will contribute and the small component will not. For the $p_{1/2}$ state the reverse will be true; the small component will contribute, while the large one will not. All other waves vanish at the origin. Nonrelativistically, only the s-waves are nonzero at the origin and all other waves vanish at the origin. The size of the $p_{1/2}$ contribution at the origin is interesting to compute in that it gives a direct measure of relativistic effects that are not included in the kinematics but are in the structure of the wave function itself and are explicitly neglected in a nonrelativistic calculation. Of course, relativistic kinematics do not suffice to reconstruct the small component. For the model we

are presently discussing the $p_{1/2}$ contribution is about 3% to 4% of the total density in O^{16} at the origin.

The parameters of the model that have to be determined are the coupling constants g_s , g_v , g_r and the mass of the sigma meson m_s . The sigma meson is taken to be the $\bar{u}\bar{d}\bar{d}$ member of the 0^{++} nonet¹⁰⁾. Its mass in the present model is determined by fitting to the surface thickness of a nucleus. The acceptable range of the mass is $500 \text{ MeV} \leq m_s \leq 525 \text{ MeV}$. A mass of 508 MeV for a zero width sigma meson is determined by fitting nucleon-nucleon phase shifts¹¹⁾. We take $m_s = 500 \text{ MeV}$ in this work. The saturation and binding energy per particle in infinite nuclear matter determine $C_s = (g_s/m_s)m_n$ and $C_v = (g_v/m_v)m_n$. For saturating Fermi momentum $k_F = 1.325 \text{ fm}^{-1}$ and binding energy per particle of -15.75 MeV and symmetry energy coefficient of 35 MeV $C_s = 18.296$, $C_v = 15.94$, $C_r = 3.5$. The values of the coupling constants thus determined are consistent with those obtained from phase shift analysis¹²⁾. The work of Miller and Green¹³⁾ and Brockmann and Weise¹⁴⁾ does not start from the saturation properties of infinite nuclear matter. The coupling constants they use lead to incorrect saturation properties of infinite nuclear matter and to incorrect density distributions in finite nuclei.

In Fig. 1 we show the proton and neutron density distributions in O^{16} , Ca^{40} , and Ca^{48} . The form factors have not been folded into the distributions. For comparison and to see how the Hartree approximation compares with Thomas-Fermi approximation we show in Fig. 2 both Hartree and T-F results for Ca^{40} for a saturating Fermi momentum of $k_F = 1.34 \text{ fm}^{-1}$ corresponding to $C_s = 17.95$ and $C_v = 15.60$. We see that the Hartree approximation improves the distributions in just the right direction. Furthermore, a comparison of Fig. 1 and Fig. 2 shows the effects of the

assumed saturating density on the predicted proton distributions. A reduction of the saturation Fermi momentum from 1.34 fm^{-1} to 1.325 fm^{-1} reduces the central density by about 7% in Ca^{40} .

The nucleus 0^{16} is of particular interest in that it has a small central depression. In the relativistic model, the central density is not given only by the the $s_{1/2}$ states but also by the small component of the $p_{1/2}$ wave function. The small component contribution can be easily seen by looking at the difference between the vector and scalar particle densities. The difference is just twice the square of the $p_{1/2}$ small component. In Fig. 3 we show the scalar and vector proton density in 0^{16} . The difference is about 8% at the origin. The $p_{1/2}$ small component fills in the depression and accounts for about 4% of the total central density. From a conventional nuclear physics point of view this is a very large contribution. The origin of this effect in the relativistic model is easily understood. The effective mass $m^* = m_n + g_s \sigma_0$ in infinite nuclear matter is $m^*/m_n = 0.56$. This small effective mass comes from the very large vector field repulsion, $g_v \omega_0 \sim 350 \text{ MeV}$, that is required to have a reasonable spin-orbit splitting in finite nuclei. Such a large reduction in the effective mass indicates that relativistic effects will be important since the relevant mass is no longer the free mass, as normally used in arguing relativistic effects, but the effective mass. In the model considered by Boguta and Bodmer $m^*/m_n \sim 0.90$ resulting in a negligible $p_{1/2}$ contribution and also in a very small spin-orbit splitting.

The above considerations show an interesting interconnection between the size of the relativistic effects, the value of m^*/m_n and the magnitude of the spin-orbit splitting. We have previously shown that the energy dependence of the optical potential¹⁵⁾ is related to these quantities. The

spin-orbit splitting can be directly obtained from the single particle eigenstates by solving the Dirac equation self-consistently. In Table 1 we show the single particle levels for O^{16} , Ca^{40} , and Ca^{48} . Here one should note the predicted $2s_{1/2}$ and $1d_{3/2}$ subshell crossing for the protons when going from Ca^{40} to Ca^{48} . Also, neutron $2s_{1/2}$ and $1d_{3/2}$ states in Ca^{48} are almost degenerate. The protons in Ca^{48} are more tightly bound than in Ca^{40} . This suggests that the proton surface thickness of Ca^{48} should be slightly smaller than that in Ca^{40} . We find this change to be about 8%. In Table 2 we show the rms radii for neutrons and protons in these nuclei. It should be noted that the eigenvalues and rms radii are somewhat dependent on the mass of the scalar meson used and the saturating density of infinite nuclear matter. For example, for $m_s = 525$ MeV, the proton rms radius in Ca^{40} is 3.345 fm while for $m_s = 500$ MeV it is 3.410 fm. As for the eigenvalues of energy, the $p_{3/2}$ eigenenergy seems to be the most sensitive one. The energy levels predicted by the model are quite good. Not so well reproduced is the total energy per particle. For Ca^{40} it is -5.7 MeV/particle for $m_s = 500$ MeV and -6.4 MeV/particle for $m_s = 525$ MeV. The deficiency of the Walecka model for the binding energy per particle in finite systems was first discussed by Boguta and Bodmer⁷⁾, where it was found that the surface energy coefficient was too large. It carries about 2 MeV/particle too much energy. That is precisely what is missing to obtain good total binding energy per particle. This situation can be easily remedied by introducing nonlinear sigma field self-interactions and slightly readjusting C_s and C_v .

From Table 2 we see that the rms radius of protons in Ca^{48} is predicted to be less than in Ca^{40} . It is interesting to know what is the role of the rho field $R_0^{(0)}$ in Ca^{48} . From eq. (7) one sees that the

rho field $R_0^{(0)}$, with $R_0^{(0)} > 0$, will decrease the energy of the protons and increase it for neutrons. That is, the protons will be attracted by the rho field, while the neutrons will be repelled. The field equation for $R_0^{(0)}$ tells us that $R_0^{(0)} \sim (\rho_V^{(n)} - \rho_V^{(p)})$. Thus, with a larger number of neutrons than protons in a nucleus, such as Ca^{48} , we obtain a larger rho field. In Fig. 4 we show the calculated rho field in Ca^{40} and Ca^{48} . For Ca^{40} the rho field is slightly negative for $r > 3.7$ fm and it actually repels protons and attracts neutrons slightly, while in Ca^{48} it is always positive and surface peaked. It will displace protons slightly inward and neutrons slightly outward. The rms radius of protons in Ca^{48} , without isospin field, is 3.39 fm. With the rho field present, it decreases to 3.359. There is a difference of about 0.03 fm. For the neutrons there is an increase in rms radius of the same size. In this model, a substantial portion of the difference in proton rms radii in Ca^{40} and Ca^{48} comes from the isospin field $R_0^{(0)}$.

TABLE 1

Single particle energy levels in O^{16} , Ca^{40} , Ca^{48}
for protons and neutrons. We list the occupied states.

	O^{16}		Ca^{40}		Ca^{48}	
	p	n	p	n	p	n
1s	34.7	38.7	46.6	53.7	51.0	57.2
1p _{3/2}	14.8	18.3	29.1	36.8	35.7	40.7
1p _{1/2}	7.7	11.3	23.9	31.5	31.2	36.4
1d _{5/2}			13.4	20.6	20.1	24.4
2s _{1/2}			7.1	14.1	11.6	16.8
1d _{3/2}			5.8	12.8	12.3	16.7
1f _{7/2}						9.35

TABLE 2

Rms radius of protons and neutrons in
 O^{16} , Ca^{40} and Ca^{48}

	r_p (fm)	r_n	$r_p - r_n$
O^{16}	2.620	2.573	0.047
Ca^{40}	3.410	3.307	0.103
Ca^{48}	3.359	3.545	-0.186

References

1. J. Boguta, Relativistic Quantum Field Theory of Finite Nuclei. LBL preprint LBL-11467
J. Boguta, Properties of $T \neq 0$ Nuclei in a Relativistic Field Theory of Nuclear Matter. LBL preprint LBL-11468
2. A. Bouyssy and X. Campi, Nukleonika, 24, 1 (1979)
3. I. Sick et al., Proc. of the Karlsruhe International Discussion Meeting, Karlsruhe, May 1979 (H. Rebel, H. J. Gils, G. Schatz, eds.), p. 97
4. X. Campi, op. cit., p. 363
5. H.-P. Duerr, Phys. Rev. 103, 469 (1956)
M.H. Johnson and E. Teller, Phys. Rev. 98, 783 (1955)
6. J.D. Walecka, Ann. Phys. 83, 491 (1974)
7. J. Boguta and A.R. Bodmer, Nucl. Phys. A292, 413 (1977)
8. S.A. Chin, Ann. Phys. 108, 491 (1977)
9. J. Boguta and J. Rafelski, Phys. Lett. 71B, 22 (1977)
10. R.L. Jaffe, Phys. Rev. D15, 267, 281 (1977)
11. M.M. Nagels et al., Phys. Rev. D12, 744 (1975)
12. M.M. Nagels, T.A. Rujken and J.J. de Swart, Phys. Rev. D17, 768 (1978)
K. Holinde and R. Machleidt, Nucl. Phys. A256, 479 (1976)
M. Lacombe, B. Loiseau, J.M. Richard, R. Vinh Mau, P. Pires and R. de Tournreil, Phys. Rev. D12, 1495 (1975)
13. L.D. Miller and A.E.S. Green, Phys. Rev. C5, 241 (1972)
14. R. Brockmann and W. Weise, Phys. Rev. 16C, 1282 (1977)

15. M. Jaminon, C. Mahaux and P. Rochus, Phys. Rev. Lett. 43, 1097 (1979)
J. Boguta, Nucleon-Nucleus Optical Potential in a Relativistic Theory
of Nuclear Matter, LBL preprint LBL-11466
L.G. Arnold, B.C. Clark and R.L. Mercer, Phys. Rev. 9C, 917 (1979)

Figure Captions

- Fig. 1a. Proton and neutron density distributions in O^{16} . The solid curve is for protons and the dashed curve for neutrons.
- Fig. 1b. Proton and neutron density distributions in Ca^{40} . The solid curve is for protons and the dashed curve for neutrons.
- Fig. 1c. Proton and neutron density distributions in Ca^{48} . The solid curve is for protons and the dashed curve for neutrons.
- Fig. 2. Comparison of Hartree and Thomas-Fermi proton distributions in Ca^{40} with $k_F = 1.34 \text{ fm}^{-1}$.
- Fig. 3. Scalar and vector proton densities in O^{16} .
- Fig. 4. Isospin on rho field $R_0^{(0)}$ in Ca^{48} and Ca^{40} . The solid curve is for Ca^{40} and dashed curve for Ca^{48} .

Fig.1a

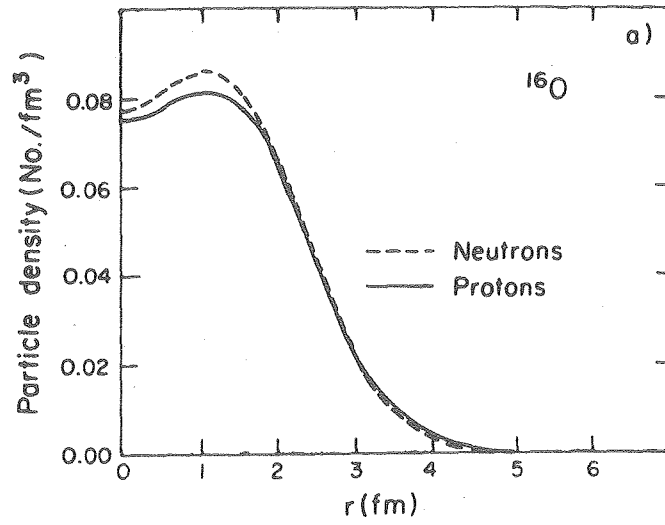


Fig.1b

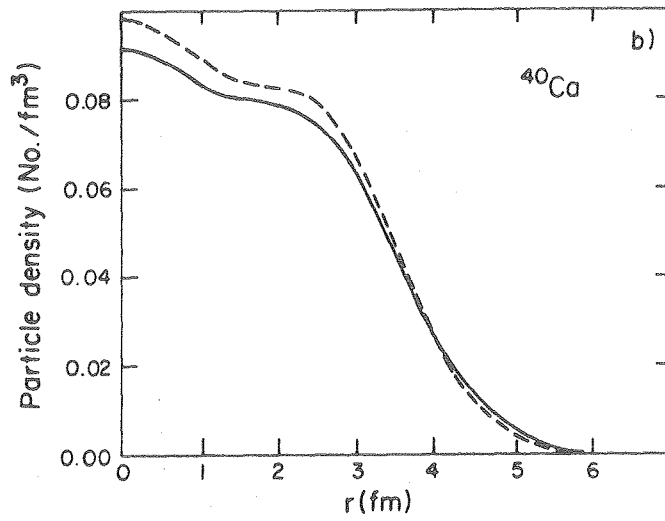
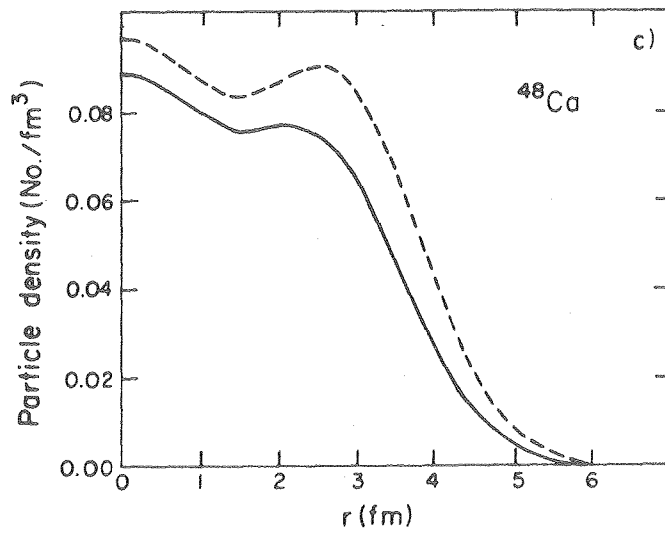
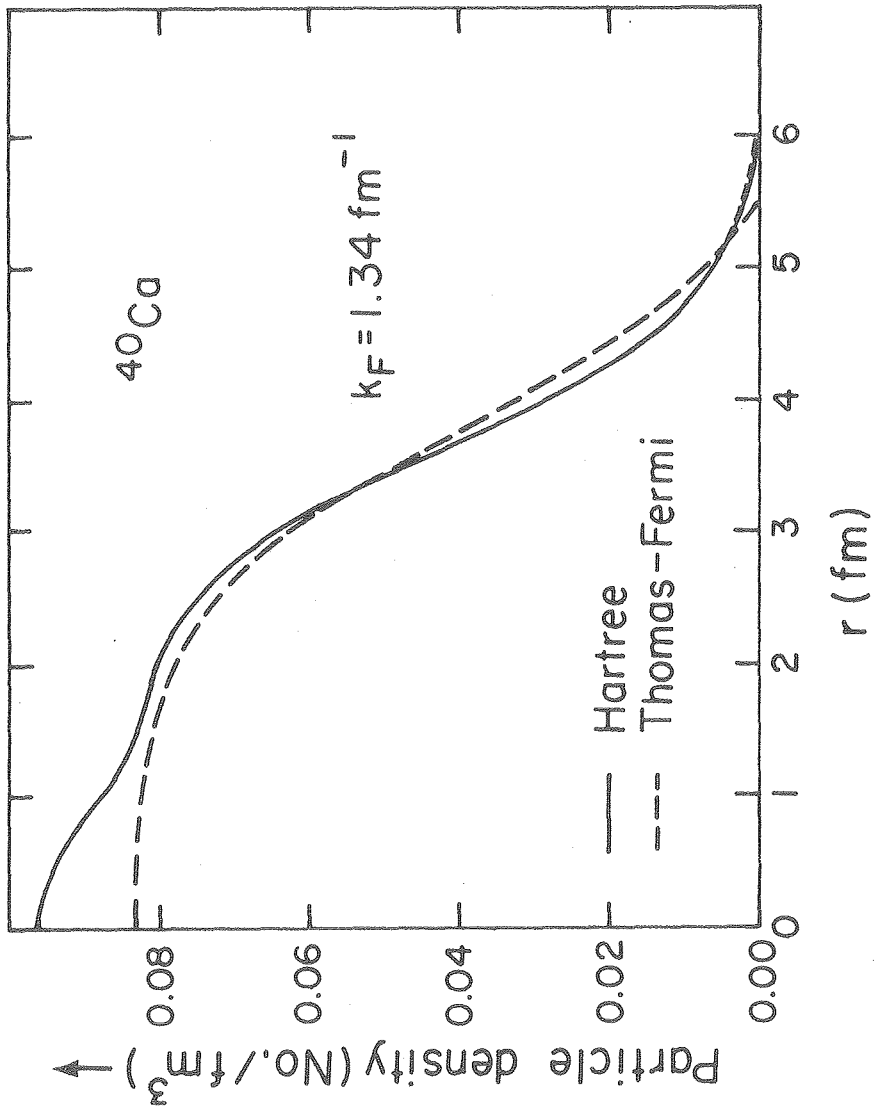


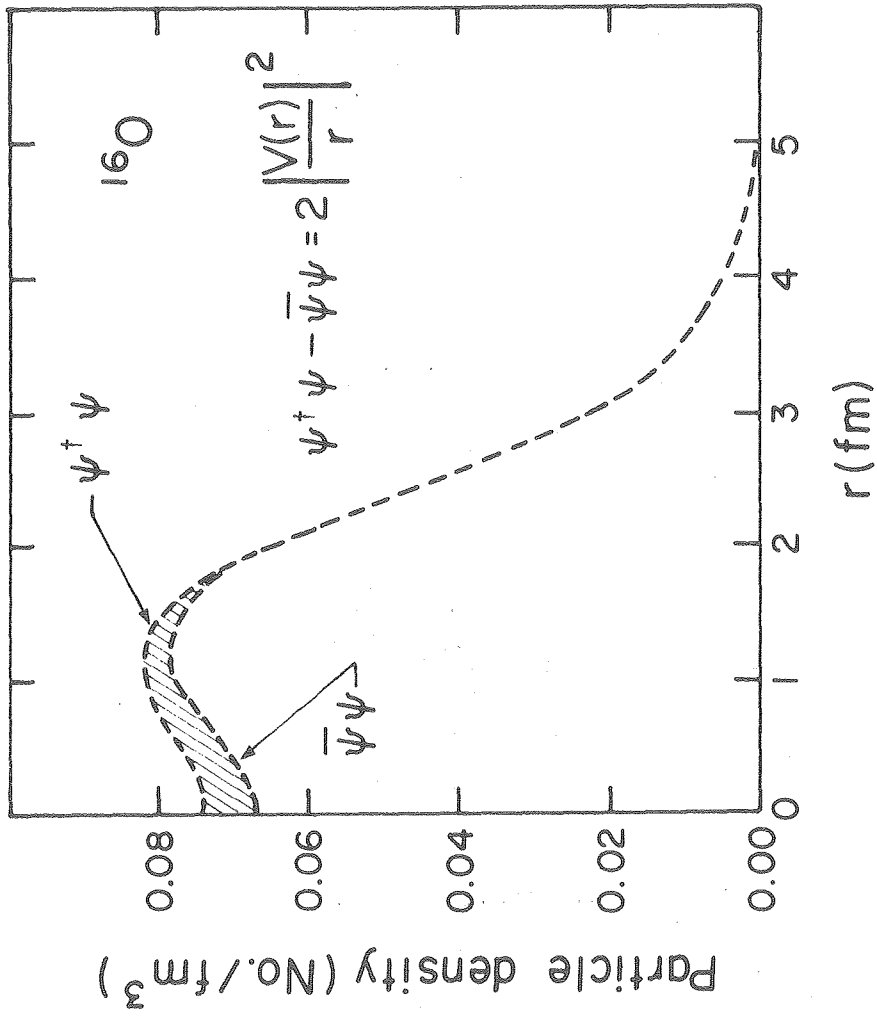
Fig.1c





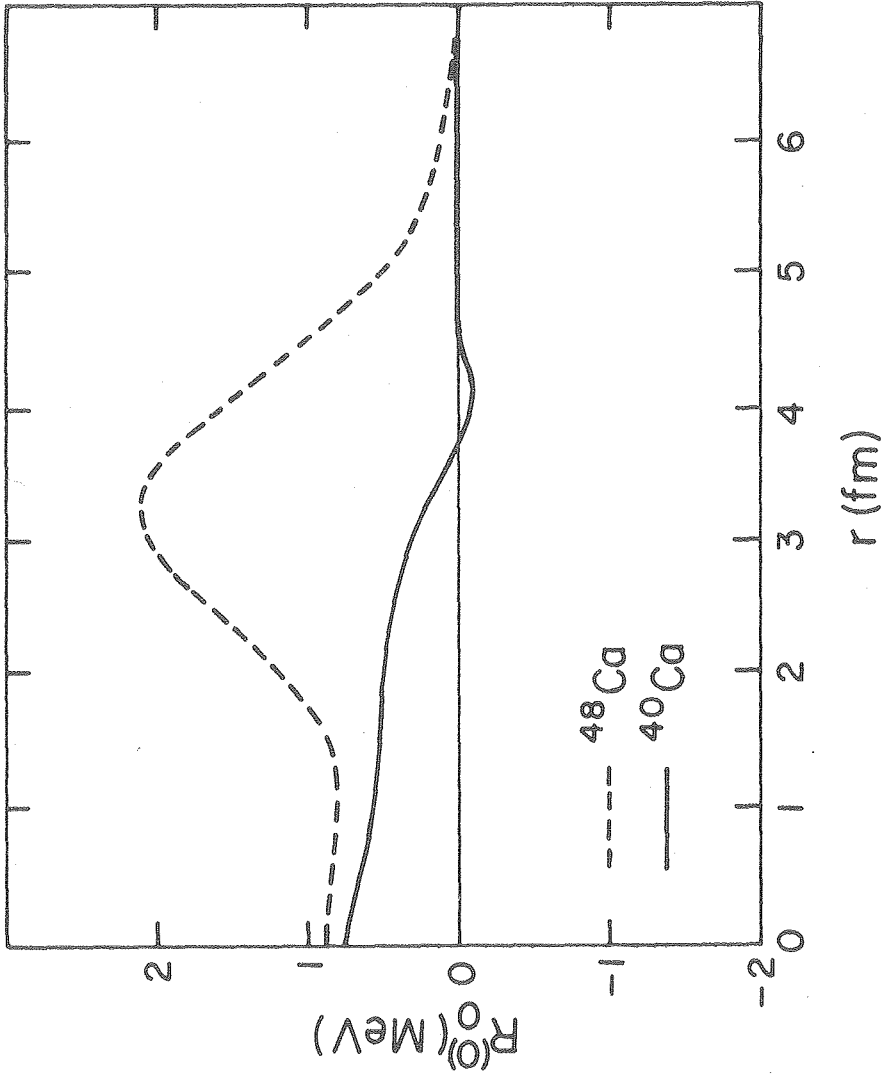
XBL 811 - 24

Fig. 2



XBL 811-25

Fig.3



XBL 811-26

Fig.4